Thin film polycrystalline Si solar cells studied in transient regime by optical pump–terahertz probe spectroscopy

P. Pikna,[1] V. Skoromets,[2] C. Becker,[3] A. Fejfar,[1] and P. Kužel[2,a)]
[1]*Institute of Physics ASCR, Cukrovarnická 10, 16253 Prague 6, Czech Republic*
[2]*Institute of Physics ASCR, Na Slovance 2, 18221 Prague 8, Czech Republic*
[3]*Helmholtz-Zentrum Berlin für Materialien und Energie GmbH, Kekuléstraße 5, 12489 Berlin, Germany*

(Received 14 October 2015; accepted 24 November 2015; published online 7 December 2015)

We used time-resolved terahertz spectroscopy to study ultrafast photoconductivity of polycrystalline thin-film silicon solar cells. We selected a series of samples, which exhibited variable conversion efficiencies due to hydrogen plasma passivation under various technological conditions. The decay of the transient terahertz conductivity shows two components: the fast one is related to the charge recombination at interfaces, while the slow nanosecond one is attributed to the trapping of photocarriers by defects localized at grain boundaries or at dislocations in the polycrystalline p^- layer of the structure. We observed a clear correlation between the open-circuit voltage and the nanosecond-scale decay time of the transient terahertz conductivity of the solar cells. Thus, the terahertz spectroscopy appears to be a useful contactless tool for inspecting the local photoconductivity of solar cells including, in particular, various nanostructured schemes. © *2015 AIP Publishing LLC*.
[http://dx.doi.org/10.1063/1.4937388]

High material quality is one of the most important preconditions for optimum conversion efficiency in solar-cell devices.[1] Good transport properties and a long lifetime of charge carriers are relevant, in particular, for the 3rd generation solar cell designs[2] based on nanostructures[3] with corresponding size effects and imperfections.[4] Electronic characterization of nanostructured materials is a challenging task, in particular, due to their variability and due to the difficulties with attaching electrical contacts to the nanoobjects.[5] The search for a suitable contact-free characterization technique appropriate for solar cells constitutes the main motivation for the present research.

In this letter, we present an investigation of thin film polycrystalline Si solar cells performed by terahertz (THz) time-resolved spectroscopy with the aim to correlate their quasi-steady-state properties with the decay times of transient THz conductivity. To establish this correlation, we study the influence of hydrogen passivation on the ultrafast dynamics of photoexcited charge carriers. The THz spectroscopy measurements are contactless and can find their use as a tool for characterization of various nanostructured solar cells prior to the electrical contact fabrication.

The performance of the studied cells is limited by their structural imperfections (e.g., grain boundaries and intra-grain defects). High density of grain boundaries and dislocations inside grains arises as a consequence of the growth of relatively small nano- to micrometer sized silicon grains during the crystallization from a solid amorphous phase (solid phase crystallization, SPC). These defects act as recombination or trapping centres for charge carriers; hydrogen plasma is used to passivate them by bonding of hydrogen radicals.[6–13] The passivation process improves the SPC solar cell conversion efficiency, but it is not sufficient to make them competitive; they were superseded by liquid-phase crystallized silicon thin films.[14,15] Nevertheless, the SPC solar cells constitute an ideal model system for the search of a correlation between the solar-cells performance and their transient conductivity obtained by quasi-optical methods. The effect of the passivation can be observed as an improvement of macroscopic quantities: the increase of the open-circuit voltage V_{OC}, the short-circuit current density J_{sc} and the fill factor.[16,17] The open-circuit voltage measured by the Suns-V_{OC} method[18] is often used as an important measure of the silicon solar-cell quality.[19,20]

The THz radiation interacts strongly with mobile conduction-band carriers in semiconductors.[21] Optical pump–THz probe experiments allow one to investigate the carrier population decay and the microscopic carrier mobility after photoexcitation; this is performed in a non-contact manner and with a ps or sub-ps time resolution.[22,23] However, the behavior of a solar cell in an impulsively driven ultrafast regime significantly differs from the usual steady-state operation. This is illustrated on the band energy structure depicted in Fig. 1. Fig. 1(a) shows the bands of a p-i-n structure under equilibrium conditions in the dark. Immediately after photoexcitation (ps to ns time scale), the excess photocarriers cause a splitting of the Fermi energy level to the quasi-Fermi levels for electrons (E_{FC}) and holes (E_{FV}) in the whole volume of the solar cell[24] (Fig. 1(b)). This state is probed by the time resolved THz spectroscopy. During the primary transport of charge carriers, the empty traps get progressively filled. The V_{OC} can be measured under quasi-steady-state conditions using a substantially longer illumination; in that case, the ultrafast transport is essentially stopped, and energetically separated Fermi levels are formed in the p^+ and n^+ films (Fig. 1(c)).[25] It is important to point out the differences in the time scales. The ultrafast THz measurements characterize the solar cell in a highly non-equilibrium regime: the sample is exposed to photon fluences of the order of 10^{12}–10^{14} photons/cm^2 within ~100 fs. Similar photon densities from the Sun are

a)Author to whom correspondence should be addressed. Electronic mail: kuzelp@fzu.cz

 © 2015 AIP Publishing LLC

This article is copyrighted as indicated in the article. Reuse of AIP content is subject to the terms at: http://scitation.aip.org/termsconditions. Downloaded to IP: 147.231.27.153 On: Mon, 07 Dec 2015 16:13:31

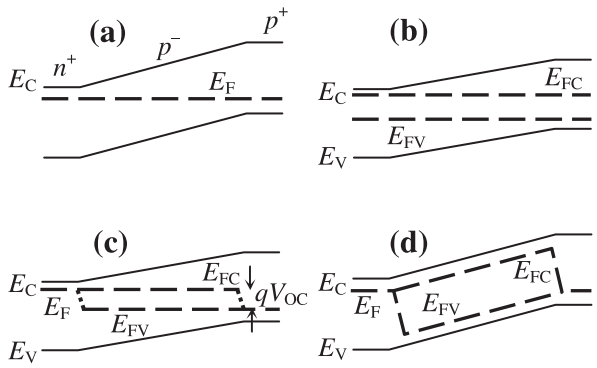

FIG. 1. Schemes of the energy band diagram of a Si p-i-n solar cell similar to those studied in this paper. (a) Equilibrium state without illumination; the space-charge region is in the p^- layer; (b) ultrafast regime immediately after pulsed photoexcitation (before the build-up of V_{OC}); (c) under steady-state illumination in the open-circuit; and (d) short-circuit conditions.

reached in the standard steady-state regime, if we integrate over units to hundreds of μs. Therefore, the photoinduced THz absorption is able to characterize processes of trapping and scattering, which are relevant for the subsequent build-up of V_{OC}.

Poly-Si thin film structures with a thickness of $\sim$1.5 μm were prepared by CSG Solar AG.[26] In brief, an amorphous Si layer with the structure $n^+/p^-/p^+$ was deposited by plasma-enhanced chemical vapor deposition on borosilicate glass coated by an antireflection SiN thin film (see Fig. 2(a)). The amorphous silicon was subsequently crystallized at 600 °C for 20 h by the SPC process forming polycrystalline silicon. Tensile stress introduced into the silicon layer by the crystallization and extended defects were eliminated by rapid thermal annealing with a short plateau phase at around 1000 °C for a few seconds. The open-circuit voltage of such as-prepared solar cells is around 230 mV.

We passivated the as-prepared structures in hydrogen plasma under various conditions. The passivation process consisted of three phases: sample heating, plateau phase, and cooling phase as schematically shown in Fig. 2(b). Unless specified explicitly, the following processing conditions were kept unchanged for all the samples: sample temperature at the plateau phase of 600 °C for an exposure of 15 min, plasma power of 50 W at a radio frequency of 13.56 MHz, and electrode distance from the sample surface of $\sim$50 mm. This combination of parameters turned out to yield relatively good and reproducible properties of the cells. The concentrations of grain boundaries and of dislocations inside the grains were typically of the order of 10^{16} cm^{-3} and 10^{10} cm^{-2}, respectively.[12]

Two series of samples were prepared. For samples of series 1, the hydrogen pressure during the passivation was kept constant at 1 mbar, while we systematically changed the temperature of plasma switch-off in the cooling phase. By optimizing this parameter, one can obtain the best compromise between the hydrogen out-diffusion from silicon (taking place if the switch-off temperature is too high) and the surface plasma damage (if the switch-off temperature is too low).[27] For passivating samples of series 2, we set the plasma switch-off temperature close to its optimum value at 343 °C and the hydrogen pressure was varied within the range of 1–3 mbar.

The thick borosilicate glass substrate absorbs rather strongly the THz radiation above 1 THz. For this reason, a Scotch® Crystal Tape was stuck to the top side of the sample

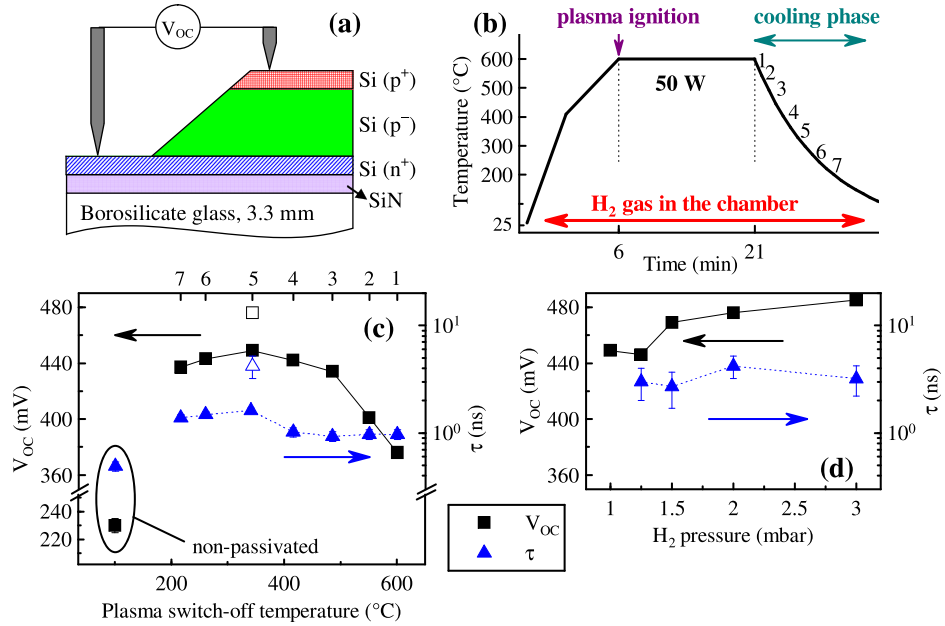

FIG. 2. (a) Structure of the studied solar cells. Nominal parameters of layers: SiN (65 nm), n^+ (50 nm, P $\approx 10^{20}$ cm^{-3}), p^- (1.4 μm, B $\approx 5 \times 10^{16}$ cm^{-3}), and p^+ (100 nm, B $\approx 2 \times 10^{19}$ cm^{-3}). Open-circuit voltage was measured by Suns-V_{OC} method using spring contacts to n^+- and p^+-doped layers. For the THz measurements, the glass substrate was etched away. (b) Temperature profile of the passivation process: the H_2 pressure and the plasma switch-off temperature (1–7) were systematically changed. (c) Dependence of open-circuit voltage V_{OC} and of carrier decay time τ on the plasma switch-off temperature, H_2 pressure: 1 mbar. Open square and triangle correspond, respectively, to V_{OC} and τ of a sample which was passivated in a 42 W plasma (instead of 50 W). (d) Dependence of open-circuit voltage and the carrier decay time on H_2 pressure for the plasma switch-off temperature of 343 °C. Note the correspondence of vertical scales in the plots (c) and (d).

This article is copyrighted as indicated in the article. Reuse of AIP content is subject to the terms at: http://scitation.aip.org/termsconditions. Downloaded to IP: 147.231.27.153 On: Mon, 07 Dec 2015 16:13:31

(p^+ Si film) and the glass substrate was removed by wet etching in 50% hydrofluoric acid at room temperature for 12 h. The whole thin-film poly-Si structure remained fixed to the tape after this procedure.

For the dynamic conductivity measurements, a custom-made setup for optical pump–THz probe experiments was used[22,28] based on a femtosecond Ti:sapphire laser amplifier (Spitfire ACE). For the optical pumping of samples, 40-fs-long pulses centered at 800 nm were used. A relatively low pump photon fluence of 5×10^{12} photons/cm^2 was employed to reach photocarrier densities of $\sim 4 \times 10^{16}\,\mathrm{cm}^{-3}$ in the p^- layer. The maximum pump-probe delay achievable in our setup is 650 ps.

Another part of the output laser beam was used for THz pulse generation and phase-sensitive detection by means of optical rectification and electro-optic gating in 1-mm-thick (110)-oriented ZnTe crystals, respectively.

An optical chopper was positioned in the path of the pump beam; this scheme ensures that we experimentally detect the photoinduced change ΔE of the THz wave form transmitted through the sample. We can safely assume that the photoinduced signal comes only from the 1.4 μm thick p^- layer (see Fig. 2(a)); the p^+ and n^+ layers are much thinner and they are highly conductive in the ground state, so that additional photocarriers with a concentration smaller than $10^{17}\,\mathrm{cm}^{-3}$ will not significantly contribute to the transient THz signal.

We checked that all the investigated samples show a Drude-like dynamical THz conductivity[28] with a dc mobility of $\mu_{dc} \sim 350\,\mathrm{cm}^2\,\mathrm{V}^{-1}\,\mathrm{s}^{-1}$ and a momentum scattering time of $\sim$60 fs. These values are about 4 times lower than those of high quality Si single crystals ($1450\,\mathrm{cm}^2\,\mathrm{V}^{-1}\,\mathrm{s}^{-1}$);[29] this demonstrates a relatively low concentration of scattering centres, i.e., a good quality of our polycrystalline layers.

Our work was mainly focused on measuring the THz transient dynamics in order to find their correlation with V_{OC}. To perform these measurements, we first found the time-domain maximum of the transient THz wave form ΔE_{max} for the pump-probe delay $\Delta t = 10$ ps. Subsequently, Δt was scanned, while the transient THz field was measured at a fixed gating time. Examples of the measured dynamics for two selected samples are shown in Fig. 3. The observed decay can be fitted by two exponentials for all the samples, which correspond to two distinct mechanisms of trapping.

The fast decay occurs in 10–20 ps range; the slow component extends on a timescale longer than 500 ps and shows a larger amplitude compared with the fast one. We can rule out a possible hypothesis of electron trapping followed by a trapping of holes as a second step of the carrier recombination, because (i) holes are much less mobile and the conductivity drop connected to their trapping would be minor and (ii) the recombination process accomplished within less than 1 ns would lead to a very poor performance of the solar cell. Thus, both decay components must be connected to distinct decay channels of mobile electrons. We can also exclude a mechanism based on two competing electron trapping channels related to various kinds of defects distributed in the bulk (such as dislocations, grain boundaries, and point defects): in this case, the two-exponential decay could be observed only if the faster channel were saturated owing to a high density of free electrons. However, the amplitude of the fast decay component scales linearly with the pump fluence (carrier density), as seen in the inset of Fig. 3. This result excludes any saturation effect. Therefore, we attribute the observed dynamics to trapping mechanisms occurring in spatially separated parts of the sample, i.e., those in the bulk and those at the interfaces. We assign the fast decay to carrier trapping at the interfaces between layers. Only a small part of carriers (those which are generated close to the interfaces) may be trapped by this mechanism in agreement with the lower amplitude of the fast component.

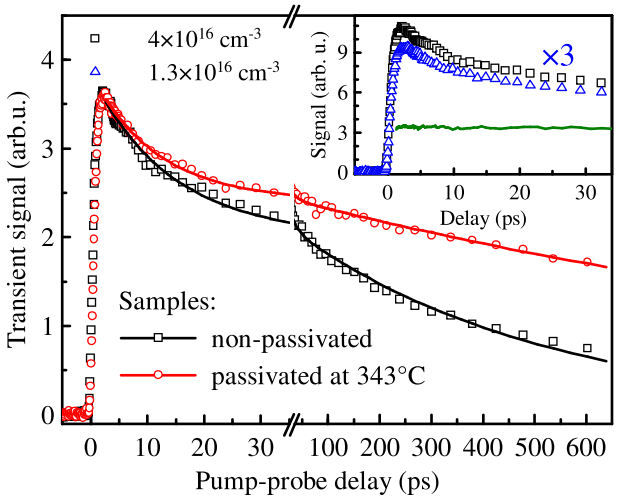

FIG. 3. Transient dynamics of two selected samples for an initial photocarrier concentration of $4 \times 10^{16}\,\mathrm{cm}^{-3}$. Symbols: experimental data and lines: bi-exponential fits. Passivation conditions of the passivated sample: plasma switch-off temperature of 343 °C and H_2 pressure of 1 mbar. Inset: symbols: measured transient dynamics of the non-passivated sample shown for two initial photocarrier concentrations and line: ratio of the two dynamics.

The time constant τ of the slow dynamical component ranges between 500 ps and a few ns. It is attributed to the carrier trapping inside the layer; therefore, it is of primary importance for our analysis. Note that, to some extent, this component can be also related to the diffusion of carriers towards the interfaces where they are eventually trapped. Indeed, the diffusion coefficient of the electrons in our sample can be estimated from their mobility using the Einstein mobility equation: $D = \mu_{dc} k_B T/e$, i.e., $D \approx 9\,\mathrm{cm}^2\,\mathrm{s}^{-1}$. The electron diffusion length $L \sim \sqrt{D\Delta t}$ then reaches about 700 nm for the time delay of $\Delta t = 600$ ps. In reality, the ambipolar diffusion will be somewhat slower due to the higher effective mass of the holes. For a non-passivated sample, the trapping process at the grain boundaries inside the p^- layer clearly dominates the transient signal (sub-ns timescale). In a perfectly passivated sample, the carrier lifetime does not exceed a few ns; we therefore think that long lifetimes in very good samples may be essentially controlled by the diffusion process.

The dependence of V_{OC} and of τ on the plasma switch-off temperature in samples from series 1 is shown in Fig. 2(c). V_{OC} increases with decreasing switch-off temperature; it reaches a maximum near 340 °C and then it starts to decrease; the non-passivated sample shows a dramatically

This article is copyrighted as indicated in the article. Reuse of AIP content is subject to the terms at: http://scitation.aip.org/termsconditions. Downloaded to IP: 147.231.27.153 On: Mon, 07 Dec 2015 16:13:31

lower V_{OC}. A similar trend is observed for τ: the non-passivated sample exhibits the shortest carrier lifetime of about 500 ps and samples with a switch-off temperature above 400 °C also show a sub-ns lifetime. In contrast, the carrier lifetime in samples with a switch-off temperature around 300 °C falls into the ns range.

Similar quantities are shown in Fig. 2(d) for samples from series 2. While V_{OC} systematically increases with H_2 pressure, no clear trend in the dependence of τ is observed. This is connected to the fact that samples prepared under these conditions are already quite optimized and the carrier lifetime increases up to several ns, for which our experimental error is relatively large. In these samples, the carrier diffusion and recombination at interfaces may dominate over the trapping in the bulk. The measured lifetime may thus depend on other details of sample preparation (thickness of p^- layer and state of the interfaces).

Fig. 4 shows a correlation plot of the carrier trapping rate $1/\tau$ against V_{OC} for all the investigated samples. A clear correlation between these two quantities is observed. We wish to stress here that the measured carrier trapping time τ is related only to the first step of the Shockley-Read-Hall recombination process (i.e., trapping at defects)[30] and it is expected to be significantly shorter than the minority carrier lifetime which is frequently used as a characteristic of solar cells. Indeed, the trapped electrons can be still thermally released back to the conduction band until they ultimately recombine through a hole trapping process, which can be rather slow in the p^- layer.

We did not observe any clear systematic dependence of the fast decay time on the experimental conditions. This fact supports also our hypothesis that the fast relaxation is related to the states at the interfaces between layers and not to those at the grain boundaries of the silicon polycrystal.

To summarize, properties of polycrystalline silicon thin-film solar cells were studied by electrical measurements and by THz spectroscopy. Although these two methods measure quite different quantities, they were both found to characterize the quality of the solar cell. Namely, we found a clear correlation between the carrier trapping rate in the bulk of the p^- layer of the solar cell and the open-circuit voltage of the solar cell structure upon systematic modifications of the H_2 passivation process of the silicon layers. The results show that the time-resolved THz spectroscopy has a potential to become a useful tool for a contactless inspection of solar cells during optimization of their properties, especially for various nanostructured configurations which often exhibit shorter lifetimes.

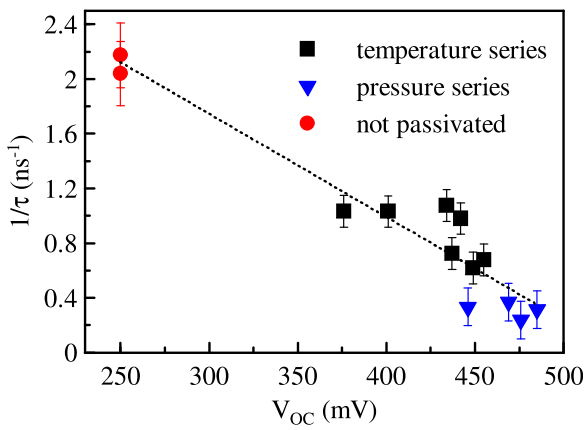

FIG. 4. Correlation between the reciprocal electron lifetime τ and the measured open-circuit voltage for all the samples studied.

We acknowledge the financial support by the Czech Science Foundation (Project No. 13-12386S). The stay of P. Pikna at Helmholtz-Zentrum was partially supported by the Project No. M100101216 of the Academy of Sciences of the Czech Republic. The German Federal Ministry of Education and Research is acknowledged for supporting C.B. within the program NanoMatFutur (No. 03X5520).

[1]R. B. Bergmann, Appl. Phys. A **69**, 187 (1999).
[2]M. A. Green, *Third Generation Photovoltaics: Advanced Solar Energy Conversion* (Springer, Berlin, 2006).
[3]J. Bisquert, *Nanostructured Energy Devices: Equilibrium Concepts and Kinetics* (CRC Press, Taylor & Francis, 2015).
[4]P. K. Nayak, G. Garcia-Belmonte, A. Kahn, J. Bisquert, and D. Cahen, Energy Environ. Sci. **5**, 6022 (2012).
[5]A. Fejfar, M. Hývl, M. Ledinský, A. Vetushka, J. Stuchlík, J. Kočka, S. Misra, B. O'Donnell, M. Foldyna, L. Yu, and P. Roca i Cabarrocas, Sol. Energy Mater. Sol. Cells **119**, 228 (2013).
[6]L. Carnel, I. Gordon, K. Van Nieuwenhuysen, D. Van Gestel, G. Beaucarne, and J. Poortmans, Thin Solid Films **487**, 147 (2005).
[7]L. Carnel, I. Gordon, D. Van Gestel, K. Van Nieuwenhuysen, G. Agostinelli, G. Beaucarne, and J. Poortmans, Thin Solid Films **511–512**, 21 (2006).
[8]B. Gorka, B. Rau, P. Dogan, C. Becker, F. Ruske, S. Gall, and B. Rech, Plasma Processes Polym. **6**, S36 (2009).
[9]M. Spiegel, C. Zechner, B. Bitnar, G. Hahn, W. Jooss, P. Fath, G. Willeke, E. Bucher, H.-U. Höfs, and C. Häßler, Sol. Energy Mater. Sol. Cells **55**, 331 (1998).
[10]G. Hahn, P. Geiger, D. Sontag, P. Fath, and E. Bucher, Sol. Energy Mater. Sol. Cells **74**, 57 (2002).
[11]D. Hiller, S. Gutsch, A. M. Hartel, P. Löper, T. Gebel, and M. Zacharias, J. Appl. Phys. **115**, 134311 (2014).
[12]S. Steffens, C. Becker, D. Amkreutz, A. Klossek, M. Kittler, Y.-Y. Chen, A. Schnegg, M. Klingsporn, D. Abou-Ras, K. Lips, and B. Rech, Appl. Phys. Lett. **105**, 022108 (2014).
[13]I. Gordon, L. Carnel, D. Van Gestel, G. Beaucarne, and J. Poortmans, Thin Solid Films **516**, 6984 (2008).
[14]C. Becker, D. Amkreutz, T. Sontheimer, V. Preidel, D. Lockau, J. Haschke, L. Jogschies, C. Klimm, J. J. Merkel, P. Plocica, S. Steffens, and B. Rech, Sol. Energy Mater. Sol. Cells **119**, 112 (2013).
[15]S. Varlamov, J. Dore, R. Evans, D. Ong, B. Eggleston, O. Kunz, U. Schubert, T. Young, J. Huang, T. Soderstrom, K. Omaki, K. Kim, A. Teal, M. Jung, J. Yun, Z. M. Pakhuruddin, R. Egan, and M. A. Green, Sol. Energy Mater. Sol. Cells **119**, 246 (2013).
[16]N. H. Nickel, N. M. Johnson, and W. B. Jackson, Appl. Phys. Lett. **62**, 3285 (1993).
[17]S. Honda, T. Mates, M. L. J. Oswald, A. Fejfar, J. K. T. Yamazaki, Y. Uraoka, and T. Fuyuki, Thin Solid Films **487**, 152 (2005).
[18]R. A. Sinton and A. Cuevas, in *16th European Photovoltaic Solar Energy Conference, Glasgow, United Kingdom*, 2000, p. 1152.
[19]M. Fehr, P. Simon, T. Sontheimer, C. Leendertz, B. Gorka, A. Schnegg, B. Rech, and K. Lips, Appl. Phys. Lett. **101**, 123904 (2012).
[20]S. Steffens, C. Becker, J.-H. Zollondz, A. Chowdhury, A. Slaoui, S. Lindekugel, U. Schubert, R. Evans, and B. Rech, Mater. Sci. Eng., B **178**, 670 (2013).
[21]R. Ulbricht, E. Hendry, J. Shan, T. F. Heinz, and M. Bonn, Rev. Mod. Phys. **83**, 543 (2011).
[22]L. Fekete, P. Kužel, H. Němec, F. Kadlec, A. Dejneka, J. Stuchlík, and A. Fejfar, Phys. Rev. B **79**, 115306 (2009).
[23]V. Zajac, H. Němec, C. Kadlec, K. Kůsová, I. Pelant, and P. Kužel, New J. Phys. **16**, 093013 (2014).
[24]C. F. Klingshirn, *Semiconductor Optics* (Springer, Berlin, 2007), p. 201.

This article is copyrighted as indicated in the article. Reuse of AIP content is subject to the terms at: http://scitation.aip.org/termsconditions. Downloaded to IP: 147.231.27.153 On: Mon, 07 Dec 2015 16:13:31

[25]J. Nelson, *The Physics of Solar Cells* (Imperial College Press, 2003), p. 145.
[26]M. J. Keevers, A. Turner, U. Schubert, P. A. Basore, and M. A. Green, in *Proceedings of the 20th European Photovoltaic Solar Energy Conference, Barcelona, Spain*, 2005, p. 1305.
[27]W. Beyer, Sol. Energy Mater. Sol. Cells **78**, 235 (2003).
[28]See supplementary material at http://dx.doi.org/10.1063/1.4937388 for details on the terahertz experimental setup and terahertz photoconductivity spectra.
[29]C. Jacoboni, C. Canali, G. Ottaviani, and A. A. Quaranta, Solid-State Electron. **20**, 77 (1977).
[30]W. Shockley and W. T. Read, Phys. Rev. **87**, 835 (1952).

This article is copyrighted as indicated in the article. Reuse of AIP content is subject to the terms at: http://scitation.aip.org/termsconditions. Downloaded to IP: 147.231.27.153 On: Mon, 07 Dec 2015 16:13:31